All-dielectric left-handed metamaterial based on dielectric resonator: design, simulation and experiment*

Yang Yi-Ming(杨一鸣)[a], Wang Jia-Fu(王甲富)[a], Xia Song(夏 颂)[b], Bai Peng(柏 鹏)[c], Li Zhe(李 哲)[c], Wang Jun(王 军)[b], Xu Zhuo(徐 卓)[b], and Qu Shao-Bo(屈绍波)[a)b)†]

[a] *College of Science, Air Force Engineering University, Xi'an* 710051, *China*
[b] *Electronic Materials Research Laboratory, Key Laboratory of the Ministry of Education, Xi'an Jiaotong University, Xi'an* 710049, *China*
[c] *Synthetic Electronic Information System Research Department, Air Force Engineering University, Xi'an* 710051, *China*

(Received 25 May 2010; revised manuscript received 22 June 2010)

Dipoles with Lorentz-type resonant electromagnetic responses can realise negative effective parameters in their negative resonant region. The electric dipole and magnetic dipole can realise, respectively, negative permittivity and negative permeability, so both the field distribution forms of electric and magnetic dipoles are fundamentals in designing left-handed metamaterial. Based on this principle, this paper studies the field distribution in high-permittivity dielectric materials. The field distributions at different resonant modes are analysed based on the dielectric resonator theory. The origination and influence factors of the electric and magnetic dipoles are confirmed. Numerical simulations indicate that by combining dielectric cubes with different sizes, the electric resonance frequency and magnetic resonance frequency can be superposed. Finally, experiments are carried out to verify the feasibility of all-dielectric left-handed metamaterial composed by this means.

Keywords: all-dielectric left-handed metamaterial, dielectric resonator, magnetic dipole, electric dipole

PACS: 41.20.Jb, 78.20.Ci, 76.20.+q, 77.84.–s **DOI:** 10.1088/1674-1056/20/1/014101

1. Introduction

In 1968, Veselago[1] theoretically investigated the characteristics of electromagnetic waves propagating in the media with both negative permittivity ε and negative permeability μ. In 1999, Pendry *et al.*[2] proposed a model of realising negative ε and negative μ. In 2000, Smith *et al.*[3] realised a 'double negative' (negative ε and negative μ) material with split rings and metal wires for the first time. Now, the research on the double-negative material which also called left-handed metamaterial has became a hot theme world-widely.

So far, the realisations of left-handed metamaterial are mostly based on the arrays built by magnetic resonators such as split-ring resonator and electric resonators such as metal wires.[4−8] All-dielectric left-handed metamaterials has also gained some profound progress. Holloway *al.*[9] proposed a method of realising electric dipole and magnetic dipole by magnetic spheres. Vendik *et al.*[10] proposed to use two set of spheres with different sizes to realise the double-negative property; Zhou and colleagues[11,12] from Tsinghua University used BST ($Ba_{0.6}Sr_{0.4}TiO_3$) ceramics with high permittivity to realise frequency-dependent negative μ and also fabricated a sandwich structure composed of ferromagnetic and dielectric materials to realise magnetically-dependent left-handed metamaterial. Compared with conventional metallic pattern-based left-handed metamaterials, all-dielectric left-handed metamaterials have much lower loss, which can be easily fabricated and are more suitable for working at high frequencies even at optical frequencies.

The field distributions of different resonant modes in different dielectric cubes were analysed by using the principle of dielectric resonators. The origination and influence factors of the electric or magnetic dipoles in dielectric resonators were studied in details. The simulation indicates that by combining cubes with different sizes, the frequencies of electric resonance and magnetic resonance can be superposed. Finally, ex-

*Project supported in part by the National Natural Science Foundation of China (Grant Nos. 50632030, 60871027 and 10804130), in part by the National Basic Research Program of China (Grant No. 2009CB613306) and the Natural Science Foundation of Shaanxi Province, China (Grant No. SJ08F01).

†Corresponding author. E-mail: qushaobo@mail.xjtu.edu.com

© 2011 Chinese Physical Society and IOP Publishing Ltd

periments were carried out to verify the feasibility of all-dielectric left-handed metamaterial composed by this means.

2. Theoretical analysis

When electromagnetic waves impinge on a single isolated sphere with a radius r_0, a relative permittivity $\varepsilon_{\rm r} = n^2$ (n is refractive index) and a permeability $\mu_{\rm r}$ which is embedded in background material with permittivity $\varepsilon_{\rm b}$ and permeability $\mu_{\rm b}$, under a plane wave illumination, the scattered fields can be decomposed into multipole terms. The m-th order electric and magnetic scattering coefficients $a_{\rm m}$ and $b_{\rm m}$ can be written as[13]

$$a_{\rm m} = \frac{n\Psi_{\rm m}(nx)\Psi'_{\rm m}(x) - \Psi_{\rm m}(x)\Psi'_{\rm m}(nx)}{n\Psi_{\rm m}(nx)\xi'_{\rm m}(x) - \xi_{\rm m}(x)\Psi'_{\rm m}(nx)}, \quad (1)$$

$$b_{\rm m} = \frac{\Psi_{\rm m}(nx)\Psi'_{\rm m}(x) - n\Psi_{\rm m}(x)\Psi'_{\rm m}(nx)}{\Psi_{\rm m}(nx)\xi'_{\rm m}(x) - n\xi_{\rm m}(x)\Psi'_{\rm m}(nx)}, \quad (2)$$

where $x = k_0 r_0$ and $k_0 = \omega/c$ is the wave vector in vacuum, $\Psi_{\rm m}$ and $\xi_{\rm m}$ are Riccati–Bessel functions.

According to Clausius–Mossotti equation,[14] when the wavelength is much larger than the dimensions of the scatterer, its effective permittivity $\varepsilon_{\rm eff}$ and effective permeability $\mu_{\rm eff}$ can be written as

$$\varepsilon_{\rm eff} = \frac{2(k_0 r_0)^3 + 6{\rm i}fa_1}{2(k_0 r_0)^3 - 3{\rm i}fa_1}, \quad (3)$$

$$\mu_{\rm eff} = \frac{2(k_0 r_0)^3 + 6{\rm i}fb_1}{2(k_0 r_0)^3 - 3{\rm i}fb_1}, \quad (4)$$

where $f = 4\pi N r_0^3/3$ and N is the number of spheres per unit volume. Based on Mie theory, we can calculate the expressions of the a_1 and b_1 from Eqs. (1) and (2),

$$a_1 = {\rm j}\frac{2}{3}(k_0^2\mu_{\rm b}\varepsilon_{\rm b})^{3/2}\frac{\varepsilon_{\rm b} - \varepsilon_{\rm r}F(\theta)}{2\varepsilon_{\rm b} + \varepsilon_{\rm r}F(\theta)}r^3, \quad (5)$$

$$b_1 = {\rm j}\frac{2}{3}(k_0^2\mu_{\rm b}\varepsilon_{\rm b})^{3/2}\frac{\mu_{\rm b} - \mu_{\rm i}F(\theta)}{2\mu_{\rm b} + \mu_{\rm i}F(\theta)}r^3, \quad (6)$$

where $F(\theta) = 2(\sin\theta - \theta\cos\theta)/[(\theta^2 - 1)\sin\theta + \theta\cos\theta]$ and $\theta = k_0 a\sqrt{\varepsilon'_{\rm r}\mu'_{\rm r}}$.

From Eqs. (3) and (4), we can see that the effective parameters of dielectric spheres are only related with its first-order electric resonance or magnetic resonance when f, r_0, N are kept unchanged.

According to the study of the Lewin,[15] based on Mie theory, we find that the effective parameters of the array composed by a set of spheres with dimensions comparable to the wavelength are frequency-dependent,

$$\varepsilon'_{\rm e} = \varepsilon_{\rm b}\left(1 + \frac{3\nu_{\rm f}}{\dfrac{F(\theta) + 2b_{\rm e}}{F(\theta) - b_{\rm e}} - \nu_{\rm f}}\right), \quad (7)$$

$$\mu'_{\rm e} = \mu_{\rm b}\left(1 + \frac{3\nu_{\rm f}}{\dfrac{F(\theta) + 2b_{\rm m}}{F(\theta) - b_{\rm m}} - \nu_{\rm f}}\right), \quad (8)$$

where $b_{\rm e} = \varepsilon_{\rm b}/\varepsilon_{\rm r}$, $b_{\rm m} = \mu_{\rm b}/\mu_{\rm r}$, $\nu_{\rm f} = 4\pi r_0^3/3p^3$, p is distance between two spheres.

As the value of $F(\theta)$ ranges theoretically from infinitesimal to infinity because of its resonant nature, it is possible to find a proper value of $F(\theta)$ to satisfy $3\nu_{\rm f}/[(F(\theta) + 2b_{\rm m})/(F(\theta) - b_{\rm m}) - \nu_{\rm f}] < -1$ or $3\nu_{\rm f}/[(F(\theta) + 2b_{\rm e})/(F(\theta) - b_{\rm e}) - \nu_{\rm f}] < -1$ to realise $\varepsilon'_{\rm e} < 0$ or $\mu'_{\rm e} < 0$.

From Eqs. (5) and (6), we see that negative ε and negative μ can be generated when the inner field of a scatterer has electric dipole and magnetic dipole, respectively, which leads to electric resonance and magnetic resonance, respectively. When a scatterer with high permittivity ($\varepsilon > 30$) works as a dielectric resonator, its first and second resonant modes have the same patterns with magnetic dipole and electric dipole, respectively. This allows us to explain the emergence of negative ε and μ in scatterers by the theory of dielectric resonators.

From the viewpoint of dielectric resonator (DR)[16] theory, the resonant nature of the dielectric sphere originates from its inner field. The dielectric particle with high permittivity can be seen as a resonator with magnetic wall. The higher the ε is, the more energy is concentrated within the particle. So the working principle of DRs is to induce electromagnetic waves into the dielectric particle, making the waves reflect between the interfaces of the dielectric and free space to form a standing wave. The radiant fields of a single DR resemble that of a electric or magnetic multdipole such as dipole, quadrupole. It is worth pointing out that this resonance can emerge not only in spheres but also other shapes. Equations (7) and (8) are only suitable for spherical DRs which is only one kind of DRs with analytical solution.

Cylinder DR, which is widely used and easily available, can generate several kinds of resonant modes such as TE (transverse electric) modes, TM (transverse magnetic) modes, HEM (hybrid electromag-

netic) modes. The first and second resonant modes are $\mathrm{HEM}_{11\delta}$ mode and $\mathrm{TM}_{01\delta}$ mode, respectively.

The qualitative relation between cylinder DR's first resonant frequency f_0 and permittivity ε_r[16] is:

$$k_0 a \propto \frac{1}{\sqrt{\varepsilon_\mathrm{r}+x}}, \tag{9}$$

where $k_0 = 2\pi f_0/c$, a is radius of cylinder, x is modified factor.

To obtain a quantitative solution, the following equations[17] must be solved:

$$h^2+\beta^2 = \varepsilon_\mathrm{r} k_0^2, \tag{10}$$

$$\frac{\mathrm{J}_0'(qa)}{q\mathrm{J}_0(qa)} + \frac{\mathrm{K}_0'(sa)}{s\mathrm{K}_0(sa)} = 0, \tag{11a}$$

$$s = \sqrt{(\varepsilon_\mathrm{r}-1)k_0^2 - q^2}, \tag{11b}$$

$$\varepsilon_\mathrm{eff} = \frac{q^2}{k^2}, \tag{12}$$

$$\frac{\mathrm{J}_0'(ha)}{h\mathrm{J}_0(ha)} + \frac{\mathrm{K}_0'(pa)}{p\mathrm{K}_0(pa)} = 0, \tag{13a}$$

$$p = \sqrt{(\varepsilon_\mathrm{eff}-1)k_0^2 - h^2}, \tag{13b}$$

$$\beta \tan\left(\frac{\beta d}{2}\right) = \alpha, \tag{14a}$$

$$\alpha = \sqrt{(\varepsilon_\mathrm{r}-1)k_0^2 - \beta^2}, \tag{14b}$$

where J_0 is the zeroth-order Bessel function of the first kind, and k_0 is the zeroth-order modified Bessel function of the second kind, k_0 is wavenumber in freespace, a is radius of the cylinder, d is height of the cylinder.

The following formula[16] can be used to estimate the first resonant frequency with accuracy about 2% when $0.5 < a/l < 2$ and $30 < \varepsilon_\mathrm{r} < 50$ (a is radius and l is height):

$$f_\mathrm{GHz} = \frac{34}{a\sqrt{\varepsilon_\mathrm{r}}}\left(\frac{a}{l}+3.45\right). \tag{15}$$

From Eq. (15), we can see that ε, a and l can affect cylinder DR's resonant frequency. The resonant frequency will decline when the height increases while the resonant mode is unchanged. But new mode will emerge and the resonant frequency will decline with the increase of the radius.

3. Simulation results and discussion

Cubic DR instead of cylinder DR is studied because it can be easily fabricated. First, a single cube to realise negative μ is considered. Figure 1(a) shows the simulation setup of a cube with sidelength $a = 4$ mm and $\varepsilon = 108$. Figure 1(b) gives its S_{21} parameter. The boundary conditions are: open boundary along x direction and electric boundaries ($E_t = 0$) along y and z directions, the port size is the same as that of a practical BJ-70 wave-guide (34.849×15.799 mm^2).

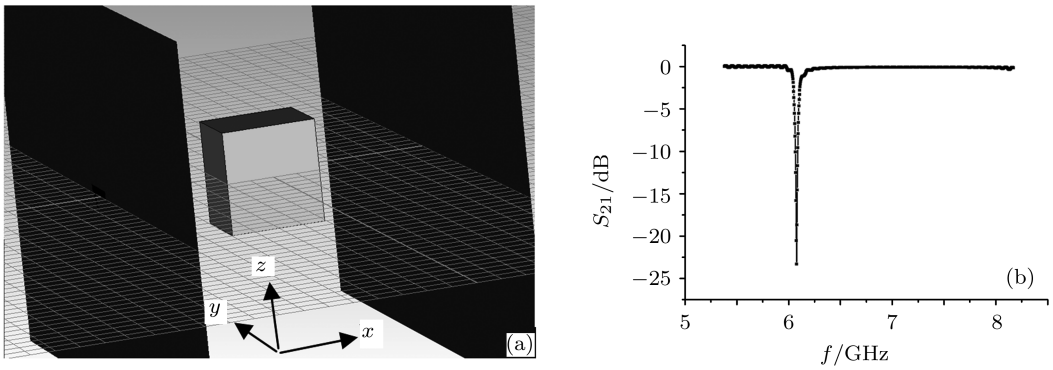


Fig. 1. Simulation of a cube with $\varepsilon = 108$ and $a = 4$ mm: (a) setup; (b) simulated S_{21} parameter.

The S_{21} minimum emerges at the frequency 6.0775 GHz in Fig. 1(b), which indicates the emergence of a resonance. The electric and magnetic fields at $f = 6.0775$ GHz are tracked in order to confirm the type of the resonance. From Fig. 2 we can see that the $\mathrm{TE}_{11\sigma}$ resonance mode emerges at $f = 6.0775$ GHz since the electric field forms a circle at the xz plane (Fig. 2(a)) and meanwhile the magnetic field at the xy plane resembles that of a magnetic dipole (Fig. 2(b)). The calculated effective μ (Fig. 2(c)) shows resonant characteristics and negative resonant region around 6 GHz. This indicates that the $\mathrm{TE}_{11\sigma}$ resonance mode can act as a magnetic dipole which can realise negative μ.

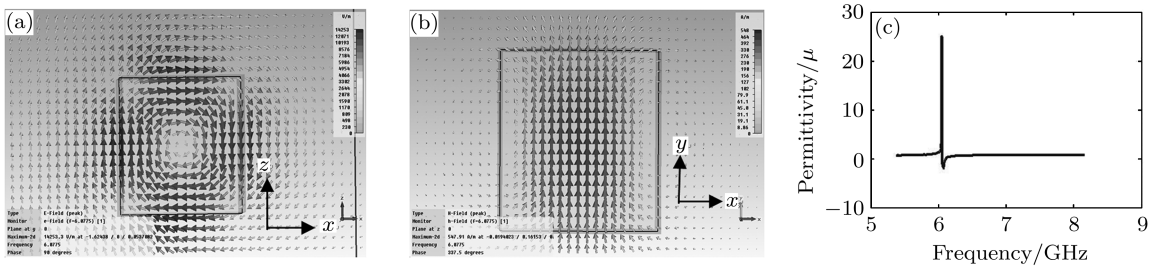


Fig. 2. Simulation of a cube with $\varepsilon = 108$ and $a = 4$ mm: (a) the electric field at $f = 6.0775$ GHz; (b) magnetic field $f = 6.0775$ GHz; (c) calculated effective μ.

According to Eq. (15), the resonance frequency will decrease when a (the sidelength of dielectric cube) increases. The electric resonance frequency is higher than the magnetic resonance frequency in dielectric cubes. By increasing a one can obtain a lower electric resonance frequency, which can make a superposition of the two different kinds of resonances. A dielectric cube with $\varepsilon = 108$ and $a = 5.5$ mm is chosen to realise electric resonance. Figures 3(a) and 3(b) give its S_{21} parameter and effective ε, respectively. As there are two resonances. The first one at $f = 6.044$ GHz is $\mathrm{TM}_{01\sigma}$ mode because of its circular magnetic field distribution (Fig. 3(c)) and electric-dipole-like electric field distribution (Fig. 3(d)). The second one at $f = 7.8994$ GHz is $\mathrm{HEM}_{21\sigma}$ mode which can be confirmed by its magnetic field pattern in Fig. 3(e). The calculated effective ε (Fig. 3(b)) also shows resonant characteristics around 6 GHz. This indicates that the $\mathrm{TM}_{11\sigma}$ mode can act as an electric dipole which can realise negative ε.

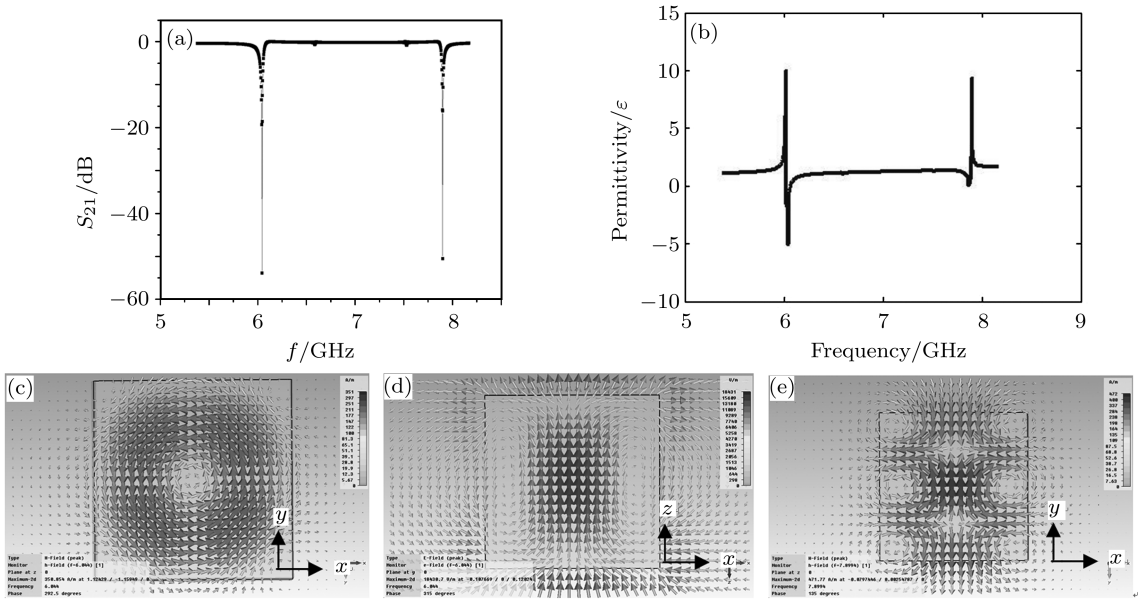


Fig. 3. Simulation of the cube with $\varepsilon = 108$ and $a = 5.5$ mm: (a) simulated S_{21} parameter; (b) calculated effective ε; (c) magnetic field at 6.044 GHz; (d) electric field at 6.044 GHz; (e) magnetic field at 7.8994 GHz.

To realise electric and magnetic resonance simultaneously, dielectric cube 1 with $\varepsilon = 108$, $a = 4$ mm and dielectric cube 2 with $\varepsilon = 108$, $a = 5.5$ mm are combined as shown in Fig. 4(a) with an interval of 4 mm between cubes. The boundary conditions and waveguide ports setup are the same as the simulation of cube $a = 4$ mm. From the comparison of the S_{21} parameters in Fig. 4(b), we can see that a pass band is formed where there is a stop band when single cube is considered around 6.1 GHz. As mentioned before, with only cube 1, a magnetic resonance will emerge due to its magnetic dipole field distribution, which leads to negative μ. With negative μ but positive ε, the electromagnetic wave will be completely reflected and a stop band in S_{21} parameter appears. For the same reason, the electric dipole formed in cube 2 around 6.1 GHz will also prevent the propagation of electromagnetic waves since it leads to negative ε. The field distributions of electric dipole and magnetic dipole exist at 6.1 GHz simultaneously by assembling two different cubes together, this fact indicates simultaneously

negative ε and μ and creates a pass band. This conclusion can also be confirmed by the calculated effective parameters in Figs. 4(c) and 4(d).

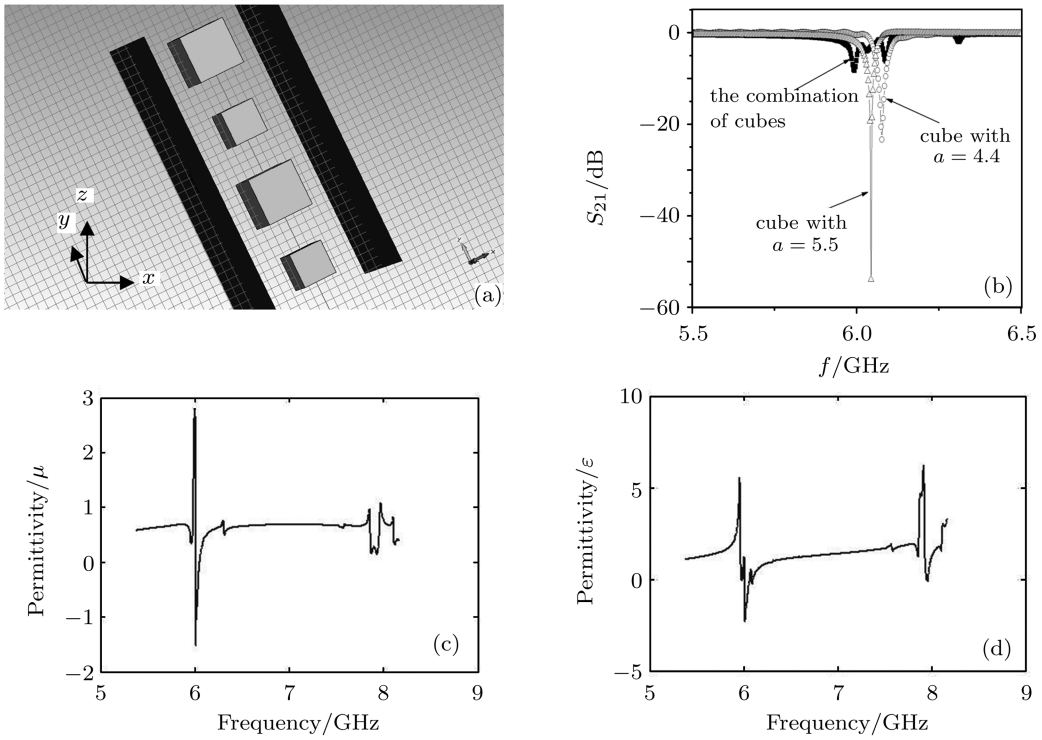
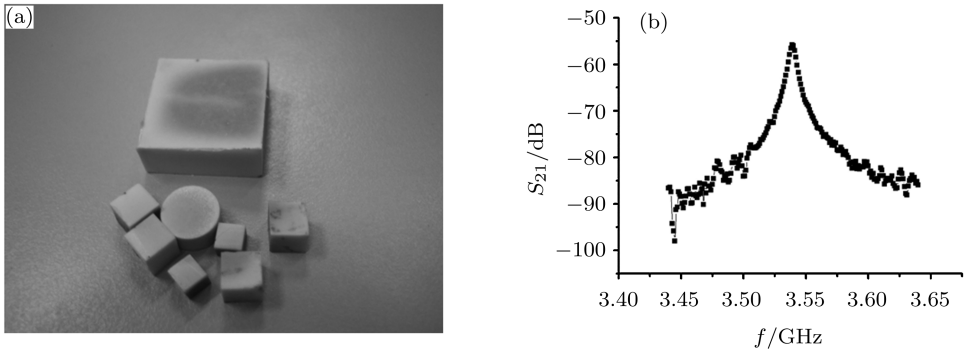


Fig. 4. Simulation of the combination of cubes of different side length: (a) setup; (b) simulated S_{21} parameters; (c) calculated effective μ; (d) calculated effective ε.

4. Fabrication of samples

The $Ba_{0.6}Sr_{0.4}TiO_3$-$La(Mg_{0.5}Ti_{0.5})O_3$ ceramic with high ε and low loss at microwave frequency is chosen to fabricate the sample. The ceramic is prepared by the following procedures: the analytical reagents of $BaCO_3$, $SrCO_3$, TiO_2, MgO, La_2O_3 are mixed according to the chemical formula $Ba_{0.6}Sr_{0.4}TiO_3$ (BST) and $La(Mg_{0.5}Ti_{0.5})O_3$ (LMT), respectively, then ball-milled for 12 hours with zirconium ball and ethanol. After dried, the BST powder and LMT powder are calcined at 1200 °C and 1400 °C for 2 hours, respectively. After BST and LMT are mixed by proper proportion, the 5% poly vinyl alcohol solution is added. Then a cylinder with height 5 mm, diameter 10 mm and a cube of 23 mm × 23 mm × 15 mm are pressed under the pressure of 20 kN and 70 kN, respectively. After PVA being burnt out at 500 °C for 3 hours, the ceramic is obtained by sintering at 1500 °C in the air for 6 hours. The cylinder is used to test its permittivity and loss at microwave frequency by using the resonant cavity method and the cube is cut into small cubes with dimensions of 5.5 mm × 5.5 mm × 5.5 mm and 4 mm × 4 mm × 4 mm to fabricate samples (Fig. 5(a)).



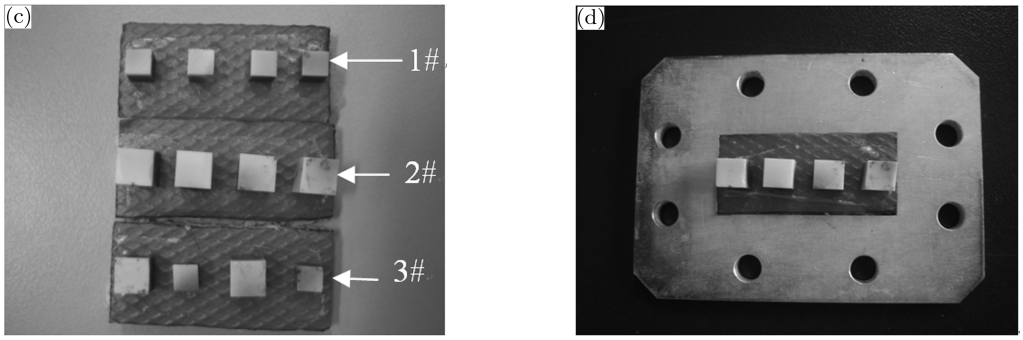


Fig. 5. (a) Sintered ceramics; (b) S_{21} parameter of cylinder ceramics tested by resonant cavity method; (c) samples tested by the wave guide method; (d) sample in waveguide.

The HP 8720ES Vector network analyser-based resonant cavity test system and wave guide test system are used to test the permittivity and loss of ceramic and S_{21} parameters of samples.

The performances of ceramics with height 4.04 mm and diameter 8.9 mm tested by resonant cavity method are (Fig. 5(b)): resonant frequency $f_0 = 3.539$ GHz, quality factor $Q = 666$, permittivity $\varepsilon = 107$, loss $\delta = 0.0016$, these performances satisfy the needs of the experiment.

5. Experiment

The testing samples are shown in Fig. 5(c). The 1# sample is composed of 4 cubes of $a = 4$ mm with interval of approximate 5 mm; the 2# sample is composed of 4 cubes of $a = 5.5$ mm with interval of approximate 3 mm; the 3# sample is composed of 2 cubes of $a = 4$ mm and 2 cubes of $a = 5.5$ mm alternately with interval of 4 mm. All samples are placed on foam substrate which has the permittivity close to 1. During the test, the wave guide of BJ-70 whose test frequency ranges from 5.38 GHz to 8.17 GHz is chosen. The way the sample are put into the waveguide is shown in Fig. 5(d).

The tested results are shown in Figs. 6(a), 6(b), 6(c) which correspond to 1#, 2#, 3# sample, respectively. From the tested results we can see that a dip emerges in 1# and 2# sample's S_{21} parameter around 6 GHz which means a stop band. A higher order resonant mode is also observed at a higher frequency in Fig. 6(b) which matches well with the simulated result. The dips mean that the magnetic and electric resonance emerge in samples 1# and 2#, respectively, which lead to negative μ and ε, respectively. By combining the two kinds of cubes together, the transmission around 6 GHz has been raised from −14–−12 dB to −4–−2 dB, which can be a reliable evidence of the existence of double- negative pass band.

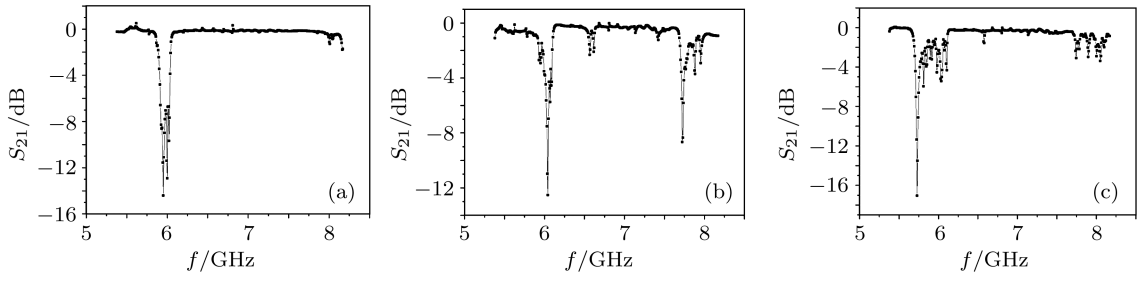


Fig. 6. Tested S_{21} parameter: (a) S_{21} parameter of sample 1#; (b) S_{21} parameter of sample 2#; (c) S_{21} parameter of sample 3#.

6. Conclusions

In this paper, a way of realising negative ε or μ by forming field distribution of electric or magnetic dipole to realise electric or magnetic resonance is proposed. A method based on dielectric resonator of explaining the electric or magnetic dipole in high-permittivity dielectric materials is proposed. Through the analysis based on dielectric resonator theory, it is found that

when the dielectric cube works at $TE_{11\delta}$ and $TM_{11\delta}$ resonant mode, it has the same field distribution with magnetic and electric dipole which can realise negative μ and ε, respectively. The resonant frequency can be changed by adjusting the dimension of the cubes. The simulated and experimental results indicate that cubes with different dimensions can realise negative μ and ε, respectively. By combining two different cubes, the frequencies of electric and magnetic resonance can be superposed to form a left-handed pass band with simultaneously negative μ and ε.

References

[1] Veselago Sov V G 1968 *Phys. Usp.* **10** 509

[2] Pendry J B, Holden A J, Robbins D J and Stewart W J 1999 *IEEE Trans. Microw. Theory Tech.* **47** 2075

[3] Smith D R, Padilla W J, Vier D C, Nemat-Nasser S C and Schultz S 2000 *Phys. Rev. Lett.* **84** 4184

[4] Xi S, Chen H, Wu B I and Kong J A 2008 *Prog. Electromagne. Res.* **84** 279

[5] Ran L, Huangfu J, Chen H, Zhang X, Cheng K, Grzegorczyk T M and Kong J A 2005 *Prog. Electromagn. Res.* **51** 249

[6] Yang Y M, Qu S B, Wang J F and Xu Z 2009 *Acta Phys. Sin.* **58** 1031 (in Chinese)

[7] Wang J F, Qu S B, Xu Z, Zhang J Q, Ma H, Yang Y M, Wu X and Lu L 2010 *Acta Phys. Sin.* **59** 4018 (in Chinese)

[8] Wang J F, Qu S B, Xu Z, Zhang J Q, Ma H, Yang Y M and Gu C 2009 *Acta Phys. Sin.* **58** 3224 (in Chinese)

[9] Holloway C L, Kuester E F, Baker-Jarvis J and Kabos P 2003 *IEEE Trans. Antennas Propag.* **51** 2596

[10] Vendik O G and Gashinova M S 2004 *34th European Microwave Conference 2004* **3** (London: Horizon House) p1209

[11] Zhao Q, Du B, Kang L, Zhao H J, Xie Q, Li B, Zhang X, Zhou J, Li L T and Meng Y G 2008 *Appl. Phys. Lett.* **92** 051106

[12] Xu F, Bai Y, Qiao L J, Zhao H J and Zhou J 2009 *Appl. Phys. Lett.* **95** 114104

[13] Bohren C F and Huffman D R 1983 *Absorption and Scattering of Light by Small Particles* (New York: Wiley-Interscience)

[14] Sihvola A 1999 *Electromagnetic Mixing Formulas and Applications, IEE Electromagnetic Waves* Ser. 47 (Stevenage, Herts, UK: The Institution of Electrical Engineers)

[15] Lewin L 1947 *Proc. Inst. Electr. Eng.* **94** 65

[16] Kajfez D and Guillon P 1998 *Dielectric Resonators* (2nd edition) (Atlanta: Noble Publishing Corporation) p9

[17] Mongia R K and Bhat B 1985 *Electron. Lett.* **21** 479